Nat. Hazards Earth Syst. Sci., 12, 1–10, 2012
www.nat-hazards-earth-syst-sci.net/12/1/2012/
doi:10.5194/nhess-12-1-2012

Natural Hazards and Earth System Sciences

Orientation effects of horizontal seismic components on longitudinal reinforcement in R/C frame elements

K. G. Kostinakis, A. M. Athanatopoulou, and I. E. Avramidis

Aristotle University of Thessaloniki, Thessaloniki, Greece

Correspondence to: A. M. Athanatopoulou (minak@civil.auth.gr)

Received: 28 February 2011 – Revised: 4 October 2011 – Accepted: 31 October 2011 – Published: 2 January 2012

Abstract. The present paper investigates the influence of the orientation of recorded horizontal ground motion components on the longitudinal reinforcement of R/C frame elements within the context of linear response history analysis. For this purpose, three single-story buildings are analyzed and designed for 13 recorded bi-directional ground motions applied along the horizontal structural axes. The analysis and design is performed for several orientations of the recording angle of the horizontal seismic components. For each orientation the longitudinal reinforcement at all critical cross sections is calculated using four methods of selecting the set of internal forces needed to compute the required reinforcement. The results show that the reinforcement calculated by three of the applied methods is significantly affected by the orientation of the recording angle of ground motion, while the fourth one leads to results which are independent of the orientation of the recording angle.

1 Introduction

Modern seismic codes (ASCE 41-06, EAK 2003, FEMA 356, FEMA P-750) suggest linear time history analysis as one of the methods that can be used for the seismic analysis and design of R/C structures. According to this method, a spatial model of the structure is analyzed using simultaneously imposed consistent pairs of earthquake records along the two horizontal structural axes (with a few exceptions, the vertical component of the ground motion is allowed to be ignored as its influence on seismic response is considered negligible). Alternatively, the structure is analyzed separately for each horizontal component, applied along each structural axis, and then the action effects are combined by the percentage (30 %) combination rule.

In most strong-motion databases, the horizontal components of the ground motion are given along the orientation they were recorded for. Thus, the orientation of the recorded seismic components is predetermined by the orientation of the recording instrument, which is in general arbitrary (Beyer and Bommer, 2007). However, the horizontal acceleration time histories are changed when they are rotated around the vertical axis or when the orientation of the sensor is changed. It has been shown (Kostinakis et al., 2009) that the structural response (i.e. axial stress at columns, bending moments at beams) is strongly affected by the recording angle of the ground motion (i.e. the orientation of the recording instrument) and the recording angle that yields the maximum response does not coincide with the orientation the accelerograms have recorded if the structural response is computed for accelerograms applied along the structural axes.

Concerning the design value of a response parameter computed by time history analysis, all seismic codes suggest that the maximum value of the response to the individual pairs is used for design if 3 pairs of accelerograms are used. If the response is computed for 7 or more records, the average of the response values to the individual records is used for design purposes. However, the codes do not clarify how we can select the sets of internal forces (response parameters) in the case that more than one response parameter is needed in order to determine the required reinforcement (e.g. the longitudinal reinforcement at a column of a R/C building).

The purpose of the present paper is to investigate the influence of the orientation of recorded horizontal ground motion components on the longitudinal reinforcement of R/C frame elements, within the framework of linear response history analysis. As seismic codes do not clearly specify how to select the set of internal forces needed to compute the columns' longitudinal reinforcement, four different methods of selection are applied. The first method, which is proposed by the authors, utilizes the simultaneous internal forces corresponding to maximum normal stresses over all seismic incident angles in every relevant cross section. Furthermore, three other methods of selecting the sectional forces, which, according to authors' opinion are compatible with code provisions, are

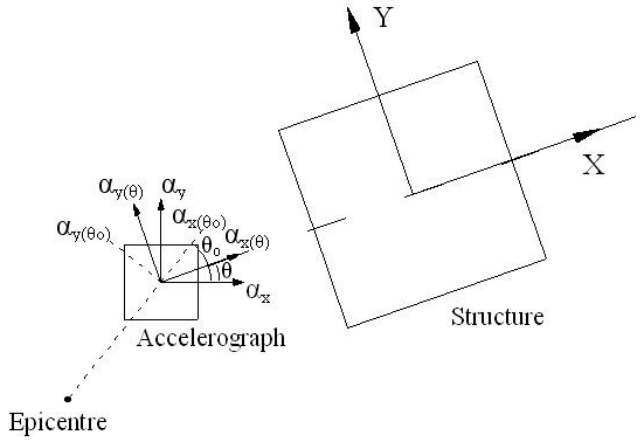

Fig. 1. Recording angle of the ground motion and orientation of building structural axes.

used. These three methods utilize the internal forces produced by accelerograms applied along the structural axes as codes specify. The first one utilizes the maximum, non-simultaneous values of internal forces, the second one the maximum values produced by 30 % rule, and the third one the simultaneous values of internal forces corresponding to maximum normal stresses (see Sect. 4) for only one orientation of accelerograms. Three single-story buildings subjected to 13 strong earthquake ground motions are analyzed and designed. The seismic motion is represented by: (i) the two horizontal recorded components; (ii) the recorded components transformed to other sets of axes forming an angle θ=30°, 60°,...,360° with respect to the initial ones and (iii) the recorded accelerograms transformed to the principal directions of the ground motion. For all these cases the longitudinal reinforcement at all critical cross sections is calculated using the four methods. The analyses results show that the reinforcement calculated by three of the applied methods is significantly affected by the orientation of the recorded ground motion components, while the fourth method leads to results which do not depend on the orientation of the seismic input.

2 Principal directions of horizontal seismic components

In most strong-motion databases, the horizontal components of the ground motion are given along the orientation they were recorded for. Thus, the orientation of the recorded seismic components is predetermined by the orientation of the recording instrument (accelerograph), which is in general arbitrary (Fig. 1).

Let α_x(t) and α_y(t) represent the recorded ground acceleration time histories at the position of the accelerograph along the axes x and y, respectively. The same ground motion can be represented by components $\alpha_{x(\theta)}$(t) and $\alpha_{y(\theta)}$(t) along another set of horizontal axes, which is defined by the angle θ with regard to the accelerograph axes x and y (Fig. 1). In other words, if the accelerograph had another orientation (e.g. x(θ), y(θ)) it would record the acceleration time histories $\alpha_{x(\theta)}$ and $\alpha_{y(\theta)}$. These components can be computed (Penzien and Watabe, 1975) with the aid of α_x and α_y by using Eq. (1):

$$\begin{bmatrix} \alpha_{x(\theta)}(t) \\ \alpha_{y(\theta)}(t) \end{bmatrix} = \begin{bmatrix} \cos\theta & \sin\theta \\ -\sin\theta & \cos\theta \end{bmatrix} \cdot \begin{bmatrix} \alpha_x(t) \\ \alpha_y(t) \end{bmatrix} \quad (1)$$

where α_x(t), α_y(t) are the recorded horizontal acceleration time histories along the axes x and y and $\alpha_{x(\theta)}$(t), $\alpha_{y(\theta)}$(t) are the components of the transformed record when rotated counterclockwise by an angle θ (Fig. 1). In general, the two components α_x, α_y or $\alpha_{x(\theta)}$, $\alpha_{y(\theta)}$ are correlated. The correlation factor ρ is given (Penzien and Watabe, 1975) by Eq. (2):

$$\rho = \frac{\sigma_{xy}}{(\sigma_{xx}\sigma_{yy})^{1/2}}, \text{ with } \sigma_{ij} = \frac{1}{s}\int_0^s \alpha_i(t)\cdot\alpha_j(t)dt; i,j = x,y \quad (2)$$

where σ_{xx}, σ_{yy} are quadratic intensities of α_x(t) and α_y(t) respectively; σ_{xy} is the corresponding cross-term; s is the duration of the motion.

There is, however, a specific set of horizontal orthogonal axes, defined by the angle θ_0 (Fig. 1), along which the correlation coefficient ρ between the horizontal components of the ground motion is zero (Penzien and Watabe, 1975). The axes specified by angle θ_0 represent the principal directions of the ground motion. The angle θ_0 is computed (Penzien and Watabe, 1975) by Eq. (3):

$$\tan 2\theta_0 = \frac{2\sigma_{xy}}{\sigma_{xx} - \sigma_{yy}}. \quad (3)$$

3 Maximum response under bi-directional excitation

The earthquake-induced translational motion at a specific point of the ground is recorded along two horizontal directions and one vertical. However, with a few exceptions, the vertical component of the ground motion is allowed to be ignored as its influence on seismic response is considered negligible. Assume a structure which is subjected to bi-directional horizontal seismic motion represented by the recorded accelerograms $\alpha_{x(\theta)}$(t) and $\alpha_{y(\theta)}$(t) along the orthogonal axes p and w. As the direction of the seismic motion is unknown, the axes p and w can form any angle θ^s with respect to the structural axes X and Y, respectively (Fig. 2a). Clearly, the structural response is a function of the seismic incident angle θ^s. Each response parameter R attains its maximum value maxR for a specific seismic incident angle θ_{cr1} (Fig. 2a). The maximum value maxR and the corresponding critical angle θ_{cr1} are computed according to the following procedure (Athanatopoulou, 2005):

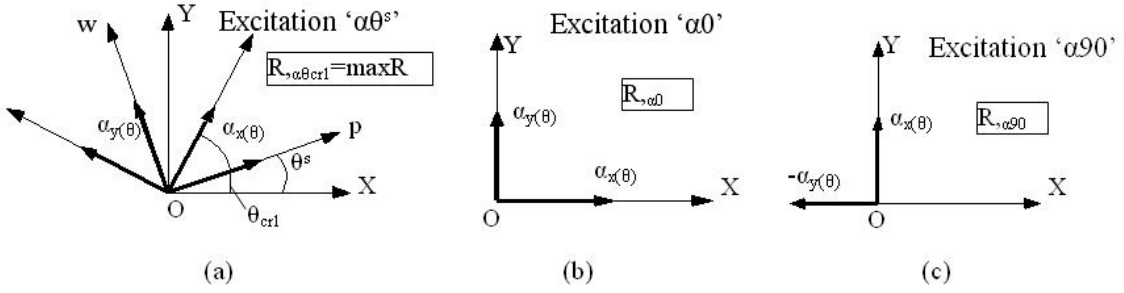

Fig. 2. Excitations "$\alpha\theta^s$", "$\alpha 0$" and "$\alpha 90$".

– Compute the response due to excitation "$\alpha 0$" (Fig. 2b): The accelerograms $\alpha_{x(\theta)}$(t) and $\alpha_{y(\theta)}$(t) are applied simultaneously along the axes X and Y, respectively, i.e. the angle of seismic incidence is θ^s=0°. A typical response quantity is denoted as $R_{,\alpha 0}$.

– Compute the response due to excitation "$\alpha 90$" (Fig. 2c): The accelerograms $\alpha_{x(\theta)}$(t) and $\alpha_{y(\theta)}$(t) are applied simultaneously along the axes Y and X, respectively, i.e. the angle of seismic incidence is $\theta^s = 90°$. A typical response quantity is denoted as $R_{,\alpha 90}$.

– The maximum value of a response parameter over all seismic incident angles is given as a function of time by Eq. (4) (Athanatopoulou, 2005):

$$R_0(t) = [R^2_{,\alpha 0}(t) + R^2_{,\alpha 90}(t)]^{1/2}. \quad (4)$$

The plot of the function $\pm R_0$(t) provides the maximum/minimum value of the required response parameter as well as the time instant t_{cr} at which this maximum/minimum occurs (Fig. 3):

$$\max R = +R_0(t_{cr}), \quad \min R = -R_0(t_{cr}). \quad (5)$$

The corresponding critical angles θ_{cr1} (maximum value) and θ_{cr2} (minimum value) are given by Eq. (6):

$$\theta_{cr1} = \tan^{-1}\left(\frac{R_{,\alpha 90}(t_{cr})}{R_{,\alpha 0}(t_{cr})}\right), \theta_{cr2} = \theta_{cr1} - \pi. \quad (6)$$

It must be noted that the maximum value maxR is computed without the previous determination of angle θ_{cr1}. Moreover, the value of any response parameter R due to seismic motion "$\alpha\theta^s$" (Fig. 2a) can be computed by the following equation (Athanatopoulou, 2005):

$$R_{,\alpha\theta^s}(t) = R_{,\alpha 0}(t) \cdot \cos\theta^s + R_{,\alpha 90}(t) \cdot \sin\theta^s. \quad (7)$$

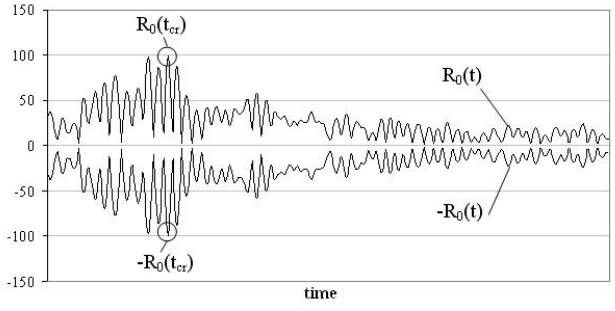

Fig. 3. Responses R_0(t) and $-R_0$(t).

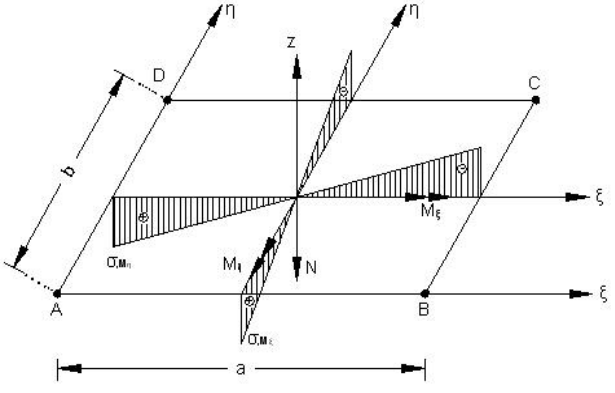

Fig. 4. Local reference system of a cross section showing internal forces and normal stresses.

4 Methods of selecting the sectional forces

In the present section, four methods of selecting the set of internal forces needed for the calculation of the longitudinal reinforcement in concrete frame elements within the context of linear response history analysis are presented. The first method is proposed by the authors since it is considered as the most rational. According to this method, the maximum axial stresses at any relevant cross section due to any incident angle of the ground motion are used in order to determine the combinations of the sectional forces required for the design of the structural elements. The axial stresses have been used in the past in order to determine the simultaneous internal

Table 1. Design combinations for method MS_{ex}.

max σ_A	N, maxσA	M$_\xi$, maxσA	M$_\eta$, maxσA
min σ_A	N, minσA	M$_\xi$, minσA	M$_\eta$, minσA
max σ_B	N, maxσB	M$_\xi$, maxσB	M$_\eta$, maxσB
min σ_B	N, minσB	M$_\xi$, minσB	M$_\eta$, minσB
max σ_C	N, maxσC	M$_\xi$, maxσC	M$_\eta$, maxσC
min σ_C	N, minσC	M$_\xi$, minσC	M$_\eta$, minσC
max σ_D	N, maxσD	M$_\xi$, maxσD	M$_\eta$, maxσD
min σ_D	N, minσD	M$_\xi$, minσD	M$_\eta$, minσD

Table 2. Design combinations for method $MF_{abs}0$.

max|N,α0|	max|M$_\xi$,α0|	max|M$_\eta$,α0|
max|N,α0|	max|M$_\xi$,α0|	−max|M$_\eta$,α0|
max|N,α0|	−max|M$_\xi$,α0|	max|M$_\eta$,α0|
max|N,α0|	−max|M$_\xi$,α0|	−max|M$_\eta$,α0|
−max|N,α0|	max|M$_\xi$,α0|	max|M$_\eta$,α0|
−max|N,α0|	max|M$_\xi$,α0|	−max|M$_\eta$,α0|
−max|N,α0|	−max|M$_\xi$,α0|	max|M$_\eta$,α0|
−max|N,α0|	−max|M$_\xi$,α0|	−max|M$_\eta$,α0|

forces needed for the design of R/C structures within the context of the response spectrum method (Gupta and Singh, 1977; Anastassiadis, 1993; Anastassiadis et al., 2002), since they were considered as the only quantity that adequately captures the response of a frame section under the simultaneous action of axial force and bending moments.

In an attempt to interpret the seismic code provisions, three other methods of selecting the sectional internal forces are used. In the following subsections, the four methods of selecting the sectional forces in R/C frame elements are presented.

4.1 Method of extreme stresses (MS_{ex})

This method (denoted in the following as MS_{ex}) is proposed by the authors and is based on the simultaneous values of internal forces corresponding to the maximum/minimum value of normal stresses occurred at a frame section for any angle of seismic incidence (Kostinakis et al., 2011). According to this method two response history analyses, under bi-directional excitation for incident angles θ^s=0° (Fig. 2b) and θ^s=90° (Fig. 2c), are performed. The time histories of the response quantities N,α0(t),M$_\xi$,α0(t) and M$_\eta$,α0(t) as well as of N,α90(t),M$_\xi$,α90(t),M$_\eta$,α90(t) at any relevant cross section are computed. Then, the time histories of the normal stresses (σ_A,α0(t), σ_B,α0(t), σ_C,α0(t), σ_D,α0(t) and σ_A, α90(t),σ_B, α90(t),σ_C,α90(t),σ_D,α90(t)) at the four corners A, B, C and D of a rectangular cross section are calculated (Fig. 4). Finally, using Eqs. (4), (5) and (6), the maximum and minimum values of the stresses, the associated critical incident angles θ_{cr1} and θ_{cr2}, as well as the time instant t_{cr} are determined. The sectional forces corresponding to these maximum and minimum values of normal stresses (determined with the aid of Eq. 7) are used for design purposes. For the four corners of a rectangular cross section, a total number of eight unfavourable combinations results.

In Table 1 the eight unfavorable combinations produced by the proposed method are presented (the term after comma denotes corresponding to). These are the most unfavourable combinations of internal forces due to seismic loads. Then the effects of the vertical and the seismic loads are added and the final unfavorable design combinations of the internal forces are obtained. These combinations are used for the calculation of the required longitudinal reinforcement. Finally, the maximum value of the 8 reinforcing steel areas produced by the sets of internal forces presented in Table 1 is selected as the required one according to the MS_{ex} method.

4.2 Method of maximum absolute forces for angle θ^s=0° ($MF_{abs}0$)

According to this method (denoted in the following as $MF_{abs}0$), the acceleration loads $\alpha_{x(\theta)}$(t) and $\alpha_{y(\theta)}$(t) are applied simultaneously along the structural axes X and Y, respectively (excitation "α0") (Fig. 2b) as codes specify. The maximum absolute values of the response parameters N,α0(t), M$_\xi$,α0(t) and M$_\eta$,α0(t) are used for design purposes. The sign of each parameter can be positive or negative. Any combination of these values can be considered as an unfavourable combination of the sectional internal forces. Hence, the eight unfavourable combinations of sectional internal forces presented in Table 2 are produced. These are the most unfavourable combinations of internal forces due to seismic loads. Then, the effects of the vertical and the seismic loads are added and the final unfavourable design combinations of the internal forces are obtained. These combinations are used for the calculation of the required longitudinal reinforcement. Finally, the maximum value of the 8 reinforcing steel areas produced by this method ($MF_{abs}0$) is selected as the required one on the basis of $MF_{abs}0$ method.

4.3 Method of 30 % rule (M30)

According to this method, two response history analyses, for uni-directional inputs $\alpha_{x(\theta)}$(t) and $\alpha_{y(\theta)}$(t) along the structural axes X and Υ, respectively, are performed. The time histories of the response quantities due to each uni-directional excitation N,$_x$(t), M$_\xi$,$_x$(t) and M$_\eta$,$_x$(t), as well as N,$_y$(t), M$_\xi$,$_y$(t), M$_\eta$,$_y$(t) (the index after comma denotes due to excitation) at any relevant cross section are computed and their maximum absolute values are determined. Then the 30 % directional combination rule is applied in order to compute the maximum response. The sets of internal forces

for design purposes according to this method for any relevant cross section are presented in Table 3.

These are the most unfavorable combinations of internal forces due to seismic loads. Then the effects of the vertical and the seismic loads are added and the final unfavourable design combinations of the internal forces are obtained. These combinations are used for the calculation of the required longitudinal reinforcement. Finally, the maximum value of the 8 reinforcing steel areas produced by the M30 method is selected as the required one for the method under consideration.

4.4 Method of extreme stresses for angle θ^s=0° ($MS_{ex}0$)

According to this method (denoted in the following as $MS_{ex}0$), the acceleration loads $\alpha_{x(\theta)}(t)$ and $\alpha_{y(\theta)}(t)$ are applied simultaneously along the structural axes X and Y, respectively (excitation "$\alpha 0$") (Fig. 2b), as codes specify, and the time histories of the normal stresses $\sigma_{A,\alpha 0}(t)$, $\sigma_{B,\alpha 0}(t)$, $\sigma_{C,\alpha 0}(t)$, $\sigma_{D,\alpha 0}(t)$ at the four corners A, B, C, and D of a rectangular cross section are computed (Fig. 4). Then, the maximum and minimum values of the stresses as well as the corresponding time instants t_1 and t_2 are determined. The sectional forces $N_{,\alpha 0}(t_i)$, $M_{\xi,\alpha 0}(t_i)$, and $M_{\eta,\alpha 0}(t_i)$ (i=1,2), corresponding to maximum and minimum values of the normal stresses, are considered for design purposes. Two unfavourable combinations of internal forces for each corner of a rectangular section are produced (one for the maximum axial stress and one for the minimum axial stress). Hence, for the four corners of the considered section, the eight unfavorable combinations shown in Table 4 are produced. These are the unfavorable combinations due to seismic loads. Then the effects of the vertical and the seismic loads are added and the final unfavorable design combinations of the internal forces are obtained. These combinations are used for the calculation of the required longitudinal reinforcement on the basis of $MS_{ex}0$ method. Finally, the maximum value of the 8 reinforcing steel areas produced by $MS_{ex}0$ method is selected as the required one for this method.

5 Structural models

Three structural models are considered in this study. Each model represents a single-story, reinforced, concrete building. The deck, rectangular in shape (L = 15 m, B = 11 m), is considered to be absolutely rigid in-plan and it is supported by four parallel plane frames in each direction (Fig. 5). The height of the story is 4 m. The concrete strength and the yield strength of the reinforcing steel are 20 MPa and 500 MPa, respectively. The modulus of elasticity is taken equal to E = 29 GPa and the damping ratio is assumed to be ζ = 5 % for all vibration modes.

The cross sectional dimensions of beams and columns are 20/50(cm) and 35/35(cm), respectively. The first model is a building with zero eccentricity ($E_s = 0$, E_s is the structural eccentricity). For each one of the other two models, it is considered that the Mass Centre CM is located on the X-axis at a distance E_s from the Centre of Stiffness CS. Regarding the mass eccentricity, two values were chosen: $e_s = E_s/L = 0.15$ and $e_s = E_s/L = 0.30$.

6 Ground motions

An ensemble of 13 pairs of horizontal ground motion records obtained from the PEER strong motion database (http://peer.berkeley.edu/smcat/) has been used as input ground motion for the analyses and design of the buildings presented in the previous section. The ground motions, which are chosen with the aid of the Appendix C of FEMA 440, have magnitudes (M_s) between 5.7 and 7.4 and are not characterized by forward-directivity effects. The motions are recorded on Soil Type B according to the classification of the Greek Seismic Code (soil type D of FEMA 356). The input ground motions are shown in Table 5 along with the critical angle of ground motion (with regard to the recorded axes) and the correlation factor of the recorded components.

The accelerograms were scaled so as to match the design spectrum of the Greek Seismic Code (EAK 2003) for Peak Ground Acceleration PGA = 0.36 g and behavior factor q = 3.5 according to the procedure suggested by ASCE 41-06. That is, each pair of accelerograms was scaled such that the SRSS of the 5 %-damped site-specific spectrum of the scaled horizontal components does not fall below 1.3 times the 5 %-damped design spectrum for periods between 0.2 T and 1.5 T (where T is the fundamental period of the building).

7 Comparative assessment of numerical results

Each one of the three models considered in the present study was analyzed using the SAP2000 for the vertical loads as well as the seismic loads. The seismic analysis was performed by linear time history analysis using the two horizontal components of the ground motions shown in Table 5. Each ground motion was represented by: (i) the two horizontal recorded components; (ii) the recorded components transformed to other sets of axes forming an angle θ=30°, 60°,...,360° with respect to the initial ones and (iii) the recorded components transformed to the principal directions of the ground motion. For all these cases, the two horizontal accelerograms were imposed simultaneously along the structural axes and the longitudinal reinforcement at all critical cross sections was calculated using the four aforementioned methods. The required reinforcement was computed according to the Greek Code for the Design and Construction of Concrete Works. The constitutive laws adopted for steel and concrete are those suggested by the Eurocode 2 and by

Table 3. Design combinations for method M30.

$\max\|N,_x\|+0.3\max\|N,_y\|$	$\max\|M_\xi,_x\|+0.3\max\|M_\xi,_y\|$	$\max\|M_\eta,_x\|+0.3\max\|M_\eta,_y\|$
$\max\|N,_x\|-0.3\max\|N,_y\|$	$\max\|M_\xi,_x\|-0.3\max\|M_\xi,_y\|$	$\max\|M_\eta,_x\|-0.3\max\|M_\eta,_y\|$
$-\max\|N,_x\|+0.3\max\|N,_y\|$	$-\max\|M_\xi,_x\|+0.3\max\|M_\xi,_y\|$	$-\max\|M_\eta,_x\|+0.3\max\|M_\eta,_y\|$
$-\max\|N,_x\|-0.3\max\|N,_y\|$	$-\max\|M_\xi,_x\|-0.3\max\|M_\xi,_y\|$	$-\max\|M_\eta,_x\|-0.3\max\|M_\eta,_y\|$
$0.3\max\|N,_x\|+\max\|N,_y\|$	$0.3\max\|M_\xi,_x\|+\max\|M_\xi,_y\|$	$0.3\max\|M_\eta,_x\|+\max\|M_\eta,_y\|$
$0.3\max\|N,_x\|-\max\|N,_y\|$	$0.3\max\|M_\xi,_x\|-\max\|M_\xi,_y\|$	$0.3\max\|M_\eta,_x\|-\max\|M_\eta,_y\|$
$-0.3\max\|N,_x\|+\max\|N,_y\|$	$-0.3\max\|M_\xi,_x\|+\max\|M_\xi,_y\|$	$-0.3\max\|M_\eta,_x\|+\max\|M_\eta,_y\|$
$-0.3\max\|N,_x\|-\max\|N,_y\|$	$-0.3\max\|M_\xi,_x\|-\max\|M_\xi,_y\|$	$-0.3\max\|M_\eta,_x\|-\max\|M_\eta,_y\|$

Table 4. Design combinations for method $MS_{ex}0$.

$\max\ \sigma_{A,\alpha0}$	N, $\max\sigma A,\alpha0$	M_ξ, $\max\sigma A,\alpha0$	M_η, $\max\sigma A,\alpha0$
$\min\ \sigma_{A,\alpha0}$	N, $\min\sigma A,\alpha0$	M_ξ, $\min\sigma A,\alpha0$	M_η, $\min\sigma A,\alpha0$
$\max\ \sigma_{B,\alpha0}$	N, $\max\sigma B,\alpha0$	M_ξ, $\max\sigma B,\alpha0$	M_η, $\max\sigma B,\alpha0$
$\min\ \sigma_{B,\alpha0}$	N, $\min\sigma B,\alpha0$	M_ξ, $\min\sigma B,\alpha0$	M_η, $\min\sigma B,\alpha0$
$\max\ \sigma_{C,\alpha0}$	N, $\max\sigma C,\alpha0$	M_ξ, $\max\sigma C,\alpha0$	M_η, $\max\sigma C,\alpha0$
$\min\ \sigma_{C,\alpha0}$	N, $\min\sigma C,\alpha0$	M_ξ, $\min\sigma C,\alpha0$	M_η, $\min\sigma C,\alpha0$
$\max\ \sigma_{D,\alpha0}$	N, $\max\sigma D,\alpha0$	M_ξ, $\max\sigma D,\alpha0$	M_η, $\max\sigma D,\alpha0$
$\min\ \sigma_{D,\alpha0}$	N, $\min\sigma D,\alpha0$	M_ξ, $\min\sigma D,\alpha0$	M_η, $\min\sigma D,\alpha0$

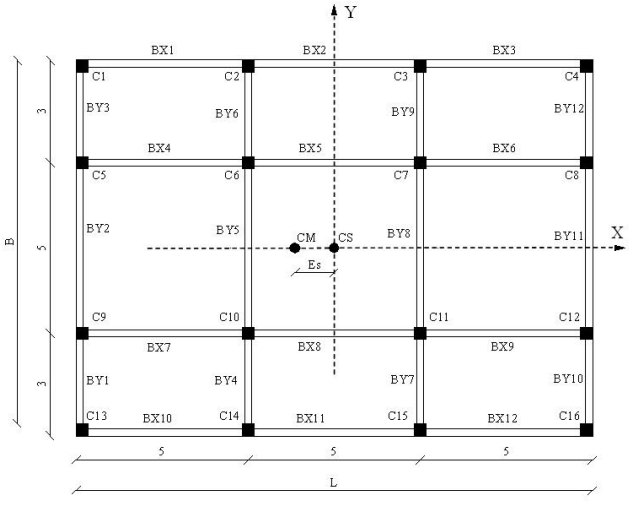

Fig. 5. Structural model (CM: Mass Centre; CS: Centre of Stiffness).

CEB-FIB. The axial load-bending moment interaction diagrams are those constructed by CEB.

Figure 6a shows the variation of the reinforcing steel ratio in column C13 bottom (Fig. 5) of the mass eccentric system ($e_s = 0.30$) under earthquake record No. 7 with respect to the recording angle. The black vertical line indicates the principal directions of the ground motion. It is evident from this figure that the reinforcement is dependent on the recording angle when methods $MS_{ex}0$, $MF_{abs}0$, and M30 are used. However, note that the required reinforcement is not influenced by the orientation of the recorded ground motion when method MS_{ex} is used because this method uses the maximum stresses over all incident angles while the rest three methods are based on response values produced by one orientation of seismic motion according to code provisions. As a consequence, method MS_{ex} produces results which are independent of the orientation of ground motion reference axes. The reinforcing steel ratio varies between 16.48 ‰ and 31.43, ‰ for method $MS_{ex}0$, between 20.63 ‰ and 35.62 ‰ for method $MF_{abs}0$, as well as between 18.00 ‰ and 31.77 ‰ for method M30. Another significant observation is that both angle $\theta = 0°$ and the angle corresponding to the principal directions of ground motion lead to much smaller reinforcement than the required reinforcement determined for other recording angles. Thus, the application of the accelerograms along the structural axes with the orientation they were recorded for, which in general is arbitrary, can significantly underestimate seismic demands.

In order to better quantify the differences among the results produced for the 12 examined orientations of the recorded ground motion, the relative variation of the reinforcing steel area for angle (θ: 0°, 30°,..., 330°) with regard to angle $\theta = 0°$ is defined as:

$$\mathrm{RV}_\theta = \frac{A_{s,\theta} - A_{s,0}}{A_{s,0}} \cdot 100(\%). \tag{8}$$

where $A_{s,\theta}$ or $A_{s,0}$: the required reinforcement for recording angle θ or (0°).

The plot of RV_θ (%) for column C13 (bottom) of the mass eccentric system (e_s=0.30) is shown in Fig. 6b. The RV_θ for method MS_{ex} is not presented in the figure, since the required reinforcement for this method is independent of the orientation of the ground motion. The maximum values of RV_θ for

Table 5. Ground motions recorded on soil type B according to Greek Seismic Code.

No	Date	Earthquake name	Magnitude (M_S)	Station name	Station number	Closest distance (Km)	Component (deg)	PGA (g)	Cor. Factor (p)	Angle θ_0
1	28/6/1992	Landers	7.4	Yermo, Fire Station	22074	24.9	270 360	0.245 0.152	−0.20	154.0
2	28/6/1992	Landers	7.4	Palm Springs, Airport	12025	37.5	0 90	0.076 0.089	0.13	60.4
3	17/1/1994	Northridge	6.7	Los Angeles, Hollywood Storage Bldg.	24303	25.5	360 90	0.358 0.231	−0.06	176.0
4	17/1/1994	Northridge	6.7	Santa Monica City Hall	24538	27.6	360 90	0.370 0.883	−0.07	94.5
5	18/10/1989	Loma Prieta	7.1	Gilroy #3, Sewage Treatment Plant	47381	14.4	0 90	0.555 0.367	0.05	5.8
6	10/1/1987	Whittier Narrows	5.7	Los Angeles, 116th St School	14403	22.5	270 360	0.294 0.396	0.01	89.2
7	10/1/1987	Whittier Narrows	5.7	Downey, Country Maintennance Bldg	14368	18.3	180 270	0.221 0.141	0.46	27.7
8	15/10/1979	Imperial Valley	6.9	El Centro #13, Strobel Residence	5059	21.9	140 230	0.117 0.139	0.12	41.6
9	15/10/1979	Imperial Valley	6.9	Calexico, Fire Station	5053	10.6	225 315	0.275 0.202	0.04	14.0
10	24/4/1984	Morgan Hill	6.1	Gilroy #7, Mantnilli Ranch, Jamison Rd	57425	14.0	0 90	0.190 0.113	0.25	28.4
11	24/4/1984	Morgan Hill	6.1	Gilroy #2, Keystone Rd	47380	15.1	0 90	0.162 0.212	0.05	83.5
12	24/4/1984	Morgan Hill	6.1	Gilroy #3, Sewage Treatment Plant	47381	14.6	0 90	0.194 0.200	0.08	46.4
13	9/2/1971	San Fernando	6.6	Los Angeles, Hollywood Storage Bldg.	135	21.2	90 180	0.210 0.174	0.18	21.9

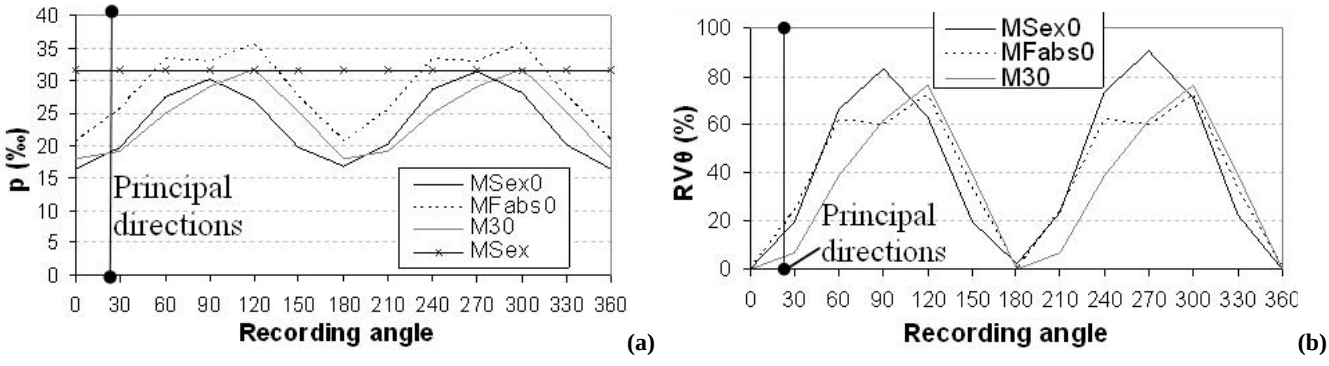

Fig. 6. Influence of the orientation of recorded ground motion **(a)** on the reinforcing steel ratios (ρ) and **(b)** on the RV_θ (%) for column C13 (bottom) of the mass eccentric system ($e_s = 0.30$) under earthquake record No. 7.

methods $MS_{ex}0$, $MF_{abs}0$, and M30 are 90.7 %, 72.7 % and 76.5 %, respectively (Fig. 6b).

The reinforcing steel ratio and the RV_θ for beam BY1top, left end (Fig. 5) of the building with zero eccentricity under earthquake No. 7 are presented in Fig. 7. We can see that the required reinforcement is strongly dependent on the recording angle when methods $MS_{ex}0$, $MF_{abs}0$, and M30 are used. As mentioned before, method MS_{ex} leads to results which are not affected by the orientation of the ground motion. It must be noted that, due to the building's symmetry, method $MF_{abs}0$ produces the same results with method M30 for all the beams of the building with zero eccentricity as well as for the parallel to Y-axis beams of the mass eccentric systems. The reinforcing steel ratio varies from 2.59 ‰ to 7.92 ‰ for method $MS_{ex}0$ and from 3.29 ‰ to 7.92 ‰ for methods $MF_{abs}0$ and M30. Of particular interest is the fact that both angle $\theta = 0°$ and the angle corresponding to the principal directions of ground motion can significantly underestimate the reinforcement with regard to the required one produced for other recording angles (Fig. 7a). The maximum

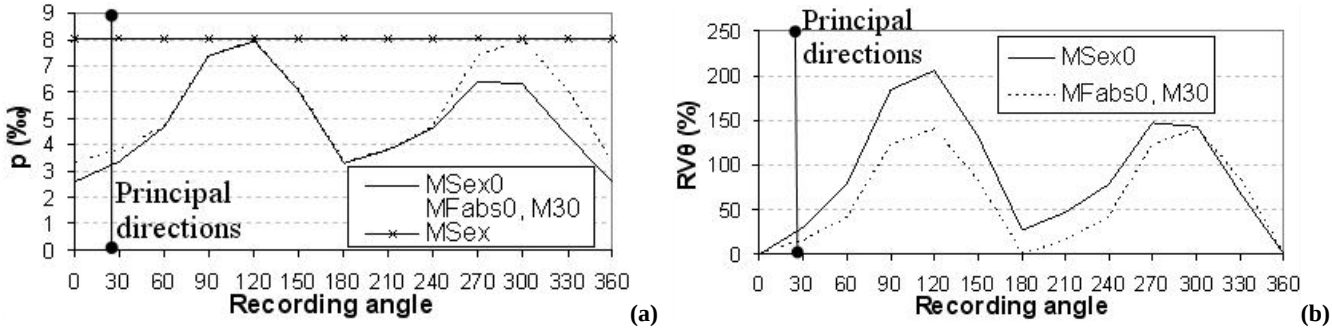

Fig. 7. Influence of the orientation of recorded ground motion **(a)** on the reinforcing steel ratios (ρ) and **(b)** on the RVθ (%) for beam BY1top (left joint) of the building with zero eccentricity under earthquake record No. 7.

values of RV$_\theta$ for methods MS$_{ex}$0, MF$_{abs}$0 and M30 are 206.1 %, 140.6 % and 140.6 %, respectively (Fig. 7b).

Furthermore, to facilitate comparisons, the Maximum Relative Variation MRV, the Maximum Relative Variation with regard to the principal directions (MRV$_{pr}$) and the Relative Variation with regard to method MS$_{ex}$ (RV$_{MSex}$) for every structural element and earthquake record are introduced:

$$\mathrm{MRV}_{,i} = \frac{\max A_{s,i} - \min A_{s,i}}{\min A_{s,i}} \cdot 100\ (\%). \quad (9)$$

$$\mathrm{MRV}_{\mathrm{pr},i} = \frac{\max A_{s,i} - A_{s,i}^{\mathrm{pr}}}{A_{s,i}^{\mathrm{pr}}} \cdot 100\ (\%). \quad (10)$$

$$\mathrm{RV}_{\mathrm{MSex},i} = \frac{A_s^{\mathrm{MSex}} - \min A_{s,i}}{A_s^{\mathrm{MSex}}} \cdot 100\ (\%). \quad (11)$$

where i: method MF$_{abs}$0, M30 or MS$_{ex}$0; max$A_{s,i}$ and min$A_{s,i}$: the maximum and the minimum reinforcement produced by method i for any recording angle θ, respectively. Moreover, $A_{s,i}^{\mathrm{pr}}$ and A_s^{MSex} are the reinforcement produced by method i using the principal components of the ground motion and the reinforcement produced by the method MS$_{ex}$, respectively.

Tables 6, 7 and 8 present the average values of MRV, MRV$_{pr}$ and RV$_{MSex}$ for all the earthquake records considered. The results are tabulated separately for each method (MF$_{abs}$0, M30 and MS$_{ex}$0) used and each examined building.

We can see (Table 6) that the average MRV can attain large values (up to 141.43 % for beam BY6top (right joint) and 108.75 % for column C12 (top)) depending on the structural element, the mass eccentricity of the building and the method used. Of particular interest is the fact that the MRV of the majority of the beams is much larger than that of the columns for the building with zero eccentricity. The above observation is valid for the 13 earthquakes and the 3 methods (MF$_{abs}$0, M30, MS$_{ex}$0) used to determine the required reinforcement. However, with increasing the mass eccentricity of the building, columns' MRV tend to become larger than beams' MRV, as the values of MRV for beams and columns exhibit opposite trends (beams' MRV decrease and columns' MRV increase).

Another significant observation is that, concerning the beams, method MS$_{ex}$0 leads to the largest values of the MRV, whereas it is not clear which is the method that produces the smallest MRV, since it depends on the mass eccentricity of the building, the structural element and the earthquake. With regard to columns, method MF$_{abs}$0 seems to produce the smallest values of MRV for the majority of the cross sections, while method MS$_{ex}$0 leads to the largest values of MRV for the mass eccentric systems.

Table 6 clearly indicates that the required reinforcement is strongly affected by the orientation of the recorded ground motion when methods MF$_{abs}$0, M30 and MS$_{ex}$0 are used to select the set of internal forces needed to determine the required reinforcement.

We can see (Table 7) that the average value of MRV$_{pr}$ corresponding to beams BX1 and BX7 is much smaller than that of beams BY6 and BY12. The same behavior pattern is observed for the vast majority of the beams which are parallel to the X structural axis regardless of the building's mass eccentricity. Moreover, Table 7 indicates that columns' MRV$_{pr}$ tend to increase as the mass eccentricity of the building increases regardless of the method used to determine the required reinforcement. The opposite trend is exhibited by the beams which are parallel to the Y structural axis.

Comparing the three methods which produce reinforcement that depends on recording angle (MS$_{ex}$0, MF$_{abs}$0 and M30), it can be concluded that regarding the beams, method MS$_{ex}$0 produces the largest while method M30 the smallest values of MRV$_{pr}$. Regarding the columns, method MS$_{ex}$0 seems to produce the largest values of MRV$_{pr}$ for the vast majority of the columns. We should recall that large MRV$_{pr}$ values indicate that the principal components of ground motion applied along the structural axes produce smaller reinforcement than the maximum one over all incident angles.

From Table 8 it can be deduced that the ratio RV$_{MSex}$ attains positive values for the vast majority of the structural elements (the only exception concerns the reinforcement of the columns of the building with zero eccentricity produced

Table 6. Average values of MRV(%) for all the earthquake records considered.

Section	e_s=0			e_s=0.15			e_s=0.30		
	$MF_{abs}0$	M30	$MS_{ex}0$	$MF_{abs}0$	M30	$MS_{ex}0$	$MF_{abs}0$	M30	$MS_{ex}0$
BX1(left)	100.74	100.74	128.29	75.84	67.54	104.80	61.38	65.51	86.14
BX1(right)	68.82	68.82	84.97	54.29	48.78	72.34	44.30	47.22	60.35
BX7(left)	96.52	96.52	121.66	84.97	81.58	116.96	72.75	80.07	95.64
BX7(right)	57.72	57.72	69.97	51.54	49.88	66.33	45.14	48.66	56.45
BY6(left)	71.65	71.65	87.94	56.73	56.73	74.90	47.22	47.22	59.40
BY6(right)	110.91	110.91	141.43	86.73	86.73	122.54	73.30	73.30	96.07
BY12(left)	80.60	80.60	100.20	49.75	49.75	62.61	36.72	36.72	45.24
BY12(right)	110.33	110.33	140.85	81.72	81.72	106.20	69.62	69.62	89.34
C1(bottom)	13.00	25.07	22.34	36.66	51.92	72.01	51.28	60.80	85.48
C1(top)	13.45	24.17	29.16	37.01	50.82	77.79	51.04	58.22	88.96
C12(bottom)	13.70	25.57	27.24	54.86	74.64	90.55	65.25	89.07	108.64
C12(top)	15.39	31.22	38.19	48.32	69.52	89.68	57.88	83.35	108.75

Table 7. Average values of MRV_{pr}(%) for all the earthquake records considered.

Section	e_s=0			e_s=0.15			e_s=0.30		
	$MF_{abs}0$	M30	$MS_{ex}0$	$MF_{abs}0$	M30	$MS_{ex}0$	$MF_{abs}0$	M30	$MS_{ex}0$
BX1(left)	7.83	7.83	17.39	12.59	6.72	19.09	19.03	7.83	23.74
BX1(right)	5.86	5.86	10.04	9.70	5.11	18.13	14.36	5.92	17.39
BX7(left)	7.73	7.73	17.20	7.73	7.16	18.09	8.90	7.46	19.79
BX7(right)	5.23	5.23	8.89	5.26	4.87	8.62	5.98	5.01	10.02
BY6(left)	63.05	63.05	69.42	51.09	51.09	54.35	40.66	40.66	46.11
BY6(right)	96.66	96.66	112.19	78.57	78.57	108.00	63.81	63.81	73.69
BY12(left)	70.66	70.66	78.23	40.57	40.57	48.52	29.26	29.26	30.53
BY12(right)	96.01	96.01	111.50	67.20	67.20	75.22	55.07	55.07	65.53
C1(bottom)	7.07	7.40	14.91	25.07	43.34	46.76	37.37	43.75	60.33
C1(top)	8.16	6.29	19.96	25.97	42.49	49.51	37.68	42.38	63.30
C12(bottom)	8.20	7.03	19.48	9.36	7.71	8.80	9.32	8.06	13.42
C12(top)	10.65	17.06	26.03	8.82	7.43	9.47	8.60	7.76	15.54

Table 8. Average values of RV_{MSex} (%) for all the earthquake records considered.

Section	e_s=0			e_s=0.15			e_s=0.30		
	$MF_{abs}0$	M30	$MS_{ex}0$	$MF_{abs}0$	M30	$MS_{ex}0$	$MF_{abs}0$	M30	$MS_{ex}0$
BX1(left)	47.22	47.22	53.28	41.98	36.63	49.40	37.61	36.57	45.60
BX1(right)	39.12	39.12	44.29	34.51	30.14	40.85	30.62	29.79	37.35
BX7(left)	46.48	46.48	52.27	43.79	42.29	50.85	40.38	41.41	46.56
BX7(right)	35.54	35.54	40.09	33.10	31.91	38.58	30.33	31.14	34.98
BY6(left)	40.39	40.39	45.35	35.23	35.23	41.34	30.41	30.41	35.54
BY6(right)	49.82	49.82	55.75	44.20	44.20	51.64	39.03	39.03	45.50
BY12(left)	25.70	25.70	30.18	31.87	31.87	37.67	42.89	42.89	48.23
BY12(right)	38.13	38.13	44.88	41.69	41.69	49.31	49.66	49.66	55.63
C1(bottom)	−5.73	26.87	18.97	19.26	35.02	41.18	23.92	36.81	44.05
C1(top)	−5.96	25.19	23.01	19.19	33.05	43.10	23.51	34.58	45.03
C12(bottom)	−6.21	27.43	21.95	20.03	36.90	43.38	29.74	41.08	48.74
C12(top)	−5.29	27.28	27.94	16.00	38.80	43.59	25.69	42.69	48.89

by method $MF_{abs}0$). This means that the reinforcement produced by accelerograms applied along the structural axes can be much smaller than the one produced by accelerograms applied along the axes which cause maximum response for the specific element and earthquake motion. The minimum reinforcement produced by methods $MF_{abs}0$, M30 and $MS_{ex}0$ can be much smaller (up to 55.75 % for beam BY6top (right joint) and 48.89 % for column C12 (top)) than the reinforcement determined by method MS_{ex}. Concerning the beams, Table 8 indicates that method $MS_{ex}0$ produces the largest values of RV_{MSex}. Furthermore, note that method $MF_{abs}0$ produces the smallest values of RV_{MSex} for all the columns of the three buildings investigated and that the values of the columns' RV_{MSex} for the three methods used tend to increase as the mass eccentricity of the building increases. It is important to notice that the above observations are valid for the vast majority of the cross sections and earthquakes considered.

8 Conclusions

In the present paper, the influence of the orientation of recorded horizontal ground motion components on reinforcement of R/C frame elements has been investigated within the framework of linear response history analysis. As existing seismic codes do not clearly specify how to select the set of internal forces for which the sections' longitudinal reinforcement should be calculated, four different methods of selection were applied. The comparative study of the results produced by the analysis and design of three illustrative examples, leads to the following conclusions:

- The reinforcement is strongly dependent on the orientation of the ground motion when methods $MS_{ex}0$, $MF_{abs}0$, and M30 are used for selecting the set of sectional forces.
- For the majority of structural elements, the application of the uncorrelated components of the ground motion along the structural axes of the building can significantly underestimate the reinforcement with regard to the reinforcement produced for other recording angles if methods $MS_{ex}0$, $MF_{abs}0$, and M30 are used.
- The influence of the recording angle on the columns' required reinforcement tends to be stronger as the mass eccentricity of the building increases. However, the opposite trend is exhibited by the vast majority of the beams of the studied buildings.
- Method MS_{ex} leads to results that are not influenced by the orientation of the recorded ground motion. This method requires the results of two bi-directional time history analyses and can be easily implemented in existing software.

Edited by: M. E. Contadakis
Reviewed by: A. Liolios and another anonymous referee

References

American Society of Civil Engineers (ASCE): Seismic Rehabilitation of Existing Buildings, ASCE 41-06, 2009.

Anastassiadis, K.: Directions sismiques de'favorables et combinaisons de'favorables des effort, Annales d l' I.T.B.T.P 512 (Mars/Avril), 83–99, 1993.

Anastasiadis, K., Avramidis, I., and Panetsos, P.: Concurrent design forces in structures under three-component orthotropic seismic excitation, Earthq. Spectra, 18, 1–17, 2002.

Athanatopoulou, A. M.: Critical orientation of three correlated seismic components, Eng. Struct., 27, 301–312, 2005.

Beyer, K. and Bommer, J. J.: Selection and scaling of real accelerograms for bi-directional loading: A review of current practice and code provisions, J. Earthq. Eng., 11, 13–45, 2007.

CEB-FIP: Manual on bending and compression–Design of sections under axial action effects at the ultimate limit state, CEB Bulletin d'Information, No. 141, Lausanne, Switzerland, 1982.

CEN 1991, Eurocode 2: Design of concrete structures. 1: General rule and rules for buildings, ENV 1992-1-1, Brussels, 1991.

EAK 2003: Greek Code for Earthquake Resistant Design of Structures, Ministry of Environment, Planning and Public Works, Greece, 2003.

EKOS 2000: Greek Code for the Design and Construction of Concrete Works, Greek Ministry of Environment, Planning and Public Works, Greece, 2000.

Federal Emergency Management Agency (FEMA): Prestandard and commentary for the seismic rehabilitation of buildings, FEMA 356, Washington, DC, 2000.

Federal Emergency Management Agency (FEMA): Improvement of nonlinear static seismic analysis procedures, FEMA 440, Washington, DC, 2004.

Federal Emergency Management Agency (FEMA): Recommended seismic provisions for new buildings and other structures, FEMA P-750 (NEHRP), Washington, DC, 2009.

Gupta, A. K. and Singh, M. P.: Design of column sections subjected to three components of earthquake, Nucl. Eng. Des., 41, 129–133, 1977.

Kostinakis, K. G., Athanatopoulou, A. M., and Avramidis, I. E.: Selection of sectional forces for designing r/c frames analysed by time history analysis, Beijing, China, in Proceedings of 14th World Conference on Earthquake Engineering, paper 08-02-0010, 2008.

Kostinakis K. G., Athanatopoulou A. M., and Avramidis I. E.: Influence of the orientation of seismic records on structural response, Bangkok, Thailand, Proceedings of IABSE Symposium, paper 051-02-01, 2009.

Kostinakis, K. G., Athanatopoulou, A. M., and Avramidis, I. E.: Sectional forces for seismic design of R/C frames by linear time history analysis and application to 3-D single-story buildings, Soil Dyn. Earthq. Eng., 31, 318–333, 2011.

Pacific Earthquake Engineering Research Center (PEER): Strong Motion Database, http://peer.berkeley.edu/smcat/, 2003.

Penzien, J. and Watane, M.: Characteristics of 3-D Earthquake Ground Motions, Earthquake Eng. Struct. Dyn., 3, 365–373, 1975.

SAP2000: Computers and Structures Inc, CSI, Berkeley, 1998.